

Published in final edited form as:

J Agric Food Chem. 2010 July 28; 58(14): 8460–8466. doi:10.1021/jf100976v.

Thionate versus Oxon: A Comparison of Stability, Uptake, and Cell Toxicity of (¹⁴CH₃O)₂-Labeled Methyl Parathion and Methyl Paraoxon with SH-SY5Y Cells

Sandip B. Bharate[†], John M. Prins[†], Kathleen M. George[†], and Charles M. Thompson^{†,§,*}

[†] The Center for Structural and Functional Neuroscience, Department of Biomedical and Pharmaceutical Sciences, The University of Montana, Missoula MT 59812

[§] ATERIS Technologies LLC, 901 N Orange Street, Missoula MT 59802

Abstract

The stability, hydrolysis and uptake of the organophosphates methyl parathion and methyl paraoxon were investigated in SH-SY5Y cells. The stabilities of (¹⁴CH₃O)₂-methyl parathion (¹⁴C-MPS) and ¹⁴C-methyl paraoxon (¹⁴C-MPO) at 1 μM in culture media had similar half lives of 91.7 h and 101.9 h, respectively. However, 100 μM MPO caused greater than 95% cytotoxicity at 24 h while 100 μM MPS caused 4–5% cytotoxicity at 24 h (~60% cytotoxicity at 48 h). Greater radioactivity was detected inside cells treated with MPO as compared to MPS although >80% of the total MPO uptake was primarily dimethyl phosphate (DMP). Maximum uptake was reached after 48 h of ¹⁴C-MPS or ¹⁴C-MPO exposure with total uptakes of 1.19 and 1.76 nM/10⁶ cells for MPS and MPO, respectively. The amounts of MPS and MPO detected in the cytosol after 48 h exposure time were 0.54 and 0.37 nM per 10⁶ cells, respectively.

Keywords

uptake; radiolabel; methyl parathion; methyl paraoxon; SH-SY5Y human neuroblastoma cells; hydrolysis; MTT

Introduction

Organophosphorus (OP) insecticides **1** are a relatively safe group of agricultural chemicals used extensively in plant and crop protection and include malathion, chlorpyrifos, parathion, methyl parathion, and diazinon (Figure 1). Most parent OP insecticides contain the phosphorothionate group (P=S), which renders the structure relatively safe to mammals owing to its poor reactivity with target enzymes and other biomolecules. The thionate linkage also confers hydrolytic stability owing to increased electron density at phosphorus. OP insecticides can be converted from thionates **1** to oxons **2** (Figure 1) either in the environment or *in vivo* and become reactive and potentially toxic following occupational or incidental exposures by direct contact with air, food and water (1). The poor reactivity of

*Communicating Author Information: Prof. Charles M. Thompson, Dept of Biomedical and Pharmaceutical Sciences, College of Health Professions and Biomedical Sciences, The University of Montana, Missoula, Montana 59812-1553, 406-243-4643 (voice); 406-243-5228 (Fax), charles.thompson@umontana.edu.

Safety. Organophosphates are toxic reagents and should be handled in a well-ventilated hood. Methyl parathion and methyl paraoxon may be rendered safe by stirring with 1 N NaOH overnight at rt.

Supporting Information Description: Radioactivity counts of OP and their degradation products in cell cytosol.

thionates is in contrast to organophosphorus warfare agents that contain the P=O linkage (oxons) and are highly reactive and induce rapid toxicity.

The primary mechanism of action of OP insecticides is based on their ability to inhibit acetylcholinesterase (AChE, EC 3.1.1.7) as the reactive oxon metabolite form **2** (Figure 1) (2). Methyl parathion (*OO*, -dimethyl *O*-4-nitrophenyl phosphorothioate) is representative of the thionates (P=S) class of insecticides with insect and mammal toxicity due to inhibition of AChE (2,3). Parathion itself is an inherently weak cholinesterase inhibitor with an IC_{50} in the range of 10^{-4} to 10^{-5} M (4) but its biotransformation to the reactive metabolite paraoxon (5–7) affords a potent inhibitor of AChE ($IC_{50} = 10^{-8}$ M) (8). Inhibition of AChE by paraoxon, as for most reactive OPs, occurs mechanistically with loss of the Z group (Figure 1) and results in accumulation of acetylcholine in cholinergic synapses, and excessive stimulation of cholinergic pathways in central and peripheral nervous systems (9–11). Although AChE is the primary target and the principle mechanism underlying toxic action, highly reactive small molecules like methyl paraoxon and ethyl paraoxon can potentially modify a number of biomolecules. Paraoxon toxicity at the cellular level has been shown in immortal cell lines *in vitro* (12–17). Subcellular targets for the initiation of cytotoxicity have not been fully elucidated but nuclear (18), enzymatic (14), cytoskeletal (19), and plasma membrane (20) alterations have been described and a number of alternative protein targets have been identified (21,22).

One significant question that remains unanswered about OP insecticide toxicity is if there are differences in the ability or rate of the structurally-similar thionate and oxon forms to penetrate cells. If this question could be answered, investigators could gain a clearer understanding of the individual or interdependent role of thionate and oxon forms of an insecticide to modify intracellular or extracellular protein targets and alter biochemical pathways that lead to toxicity. Since the conversion of thionate to oxon occurs with most thionate OP insecticides, the study of cell membrane penetration is of broad and significant impact. A differential study of cell penetration is further warranted to address a number of hypotheses regarding cell culture studies with various thionate-oxon structures. For example, toxic effects due to OP exposure likely begin with covalent modification (adduction) of a protein by the oxon (21). Owing to the relatively high reactivity and hydrolytic instability it is presumed that OP oxons would not be found at appreciable concentrations within cells as compared to the thionate owing to lower lipophilicity. Support for this supposition is indicated in calculations of partition coefficients in which methyl parathion ($CLogP = 2.79$; $\log P_{o/w} = 3.0$) (23) and methyl paraoxon ($CLogP = 1.38$; $\log P_{o/w} = 1.6$ for ethyl paraoxon) (24) show a 20-fold difference suggesting that the thionate could more readily penetrate cell membranes by passive diffusion mechanisms. However, alternative mechanisms could enable oxons access to intracellular targets.

Given the reactivity, aqueous instability and lower $ClogP$ of oxons as compared to thionates, it has been presumed that cell penetration is somewhat limited. However, it is important to recognize that OP insecticide toxicity represents exposure to both thionate and oxon forms and an understanding of cell penetration by these structures is important to validate and identify new protein targets, their localization and distribution. Moreover, the fractional concentration of extracellular and intracellular amounts of thionate and oxon may play an important role in the mode of toxic action. In this paper, the stability, uptake and hydrolysis of doubly-labeled methyl parathion and methyl paraoxon was conducted in SH-SY5Y cells so that the key structural difference between OP insecticide (thionate) and its primary metabolite (oxon) could be better understood. Rationale for the double label was two-fold: (1) placement of radiolabel at the methoxy group ensures that the isotope would remain attached to proteins since the *p*-nitrophenoxy group is lost upon phosphorylation, and (2) two methoxy ester radiolabels were deemed important since some proteins or biomolecules

may be prone to aging or loss of a second ester group following phosphorylation. The SH-SY5Y cell line was chosen for study because it expresses AChE, a number of neuron-specific enzymes and biosynthetic pathways, dopamine hydroxylase, tyrosine hydroxylase, aromatic L-amino acid decarboxylase, enzymes unique to catecholamine neurons, and the nicotinic acetylcholine receptor (25).

Materials and Methods

General

¹⁴C-Methyl parathion (¹⁴C-MPS) was purchased from Perkin-Elmer, Boston (NEN[®] radiochemicals) with a radioactivity of 1 mCi (specific activity 41.65 mCi/mmol). Liquid scintillation counting (LSC) was performed to determine the radiocarbon content of various samples using a Tricarb 2900 liquid scintillation counter, USA. Silica gel G₂₅₄ thin layer chromatography plates (10 mm thickness; Analtech) were used for purification. Radioactive images of TLC plates were recorded using a phosphoimager (Fujifilm FLA3000). The MTT assay kit was obtained from Roche Applied Science and the absorbance was measured using a microplate reader (Molecular Devices, Versamax).

Synthesis of ¹⁴C-Methyl Paraoxon (¹⁴C-MPO)

¹⁴C-Methyl paraoxon (¹⁴C-MPO) was prepared by oxidation of ¹⁴C-methyl parathion (¹⁴C-MPS). To a solution of ¹⁴C-MPS (1 mCi with a specific activity of 41.65 mCi/mmol) in dry methylene chloride (3 mL) was added meta-chloroperoxybenzoic acid (1.5 mmol) at 0 °C and the reaction mixture was stirred at rt for 2 h or until completion of reaction was confirmed by TLC. The reaction mixture was loaded onto a preparative silica gel G₂₅₄ TLC plate and eluted with EtOAc/hex (1:1). The band of ¹⁴C-MPO at R_f 0.15–0.20 (R_f of ¹⁴C-MPS is 0.60–0.65) was correlated with the migration of cold paraoxon standard, removed, extracted with methylene chloride (5 mL × 3), filtered and the solvent evaporated to afford the radiolabeled product (0.360 mCi with a specific activity of 41.65 mCi/mmol). Total counts (cpm) were converted to dpm using: dpm = cpm/detector efficiency. The radiochemical yield of synthesized ¹⁴C-MPO was determined using this relationship: 1 mCi = 2.2 × 10⁹ dpm. Chemical and radiochemical purity for both ¹⁴C-methyl parathion and ¹⁴C-methyl paraoxon were >98% based on total recovery from the TLC plate (Figure 2).

SH-SY5Y Cell Culture

SH-SY5Y cells (a human neuroblastoma cell line) were obtained from American Type Culture Collection (Rockville, MD) and cultured in DMEM/F12 medium (GIBCO BRL, Grand Island, NY) supplemented with 10% fetal bovine serum (Hyclone), 100 U/mL penicillin, 100 µg/mL streptomycin, and 2 mM L-glutamine in a CO₂ incubator maintained at 5% CO₂ and 37 °C. The medium was changed every two days. Cells were allowed to reach 80% confluence before exposure to ¹⁴C-MPS or ¹⁴C-MPO.

3-(4,5-Dimethylthiazol-2-yl)-2,5-diphenyltetrazolium bromide (MTT) Viability Assay

Approximately, 0.25 × 10⁵ cells/well were seeded into 96 well plates and exposed for 24, 48, or 72 h to MPS and MPO at concentrations from 10 nM to 100 µM prepared as solutions in acetonitrile (0.1% v/v). A 2% Triton X-100 solution in assay medium was used for a positive control (n = 8 for each MPS and MPO concentration and Triton X-100). Following exposure, cells were rinsed several times with culture medium prior to MPS and MPO exposure. Culture medium was removed and 100 µl of fresh medium containing the graded MPS and MPO concentrations or Triton X-100 was added to each well. After incubation for appropriate time points, 10 µl of MTT labeling reagent was added to each well. Plates were incubated with MTT labeling reagent for 4 h and then 100 µl of solubilizing solution was

added to each well and incubated overnight. Absorbance of samples was measured using a microplate reader at 575 nm (formazan) using a reference wavelength at 675 nm. Viability was determined by comparing the absorbance readings of the wells containing the OP-treated cells with those of the vehicle (0.1% acetonitrile) treated cells (Figure 3).

Stability of ^{14}C -MPS and ^{14}C -MPO in Culture Media

A 1 μM solution of ^{14}C -MPS or ^{14}C -MPO in DMEM/F12 medium 1% fetal bovine serum (Hyclone; 100U/mL penicillin, 100 $\mu\text{g}/\text{mL}$ streptomycin, and 2 mM L-glutamine) was incubated at 37 $^{\circ}\text{C}$ for 120 h. At different time points (0 to 120 h), samples (50 $\mu\text{l} \times 3$) were loaded onto preparative silica gel G_{254} TLC plates and developed with EtOAc: hex (1:1). Cold MPS and MPO were spotted as elution standards at the corner of the plate for reference. For ^{14}C -MPS, three bands ($R_f = 0.62, 0.15$ and < 0.1) and for ^{14}C -MPO, two bands ($R_f = 0.15$ and < 0.1) were isolated, and the total counts (cpm) recorded. The percentage of ^{14}C -MPS or ^{14}C -MPO at each time point was calculated and plotted against incubation time (Figure 4). Rate constants for the degradation of MPS and MPO were determined by calculating the negative slope of $\ln(\%$ of MPS/MPO remaining) vs. incubation time.

Uptake of ^{14}C -MPS and ^{14}C -MPO in SH-SY5Y Cells

^{14}C -MPS and ^{14}C -MPO stock solutions were prepared in acetonitrile (500 μM) and stored at 0 $^{\circ}\text{C}$. ^{14}C -MPS and ^{14}C -MPO treatment concentrations (1 μM) were prepared by dilution of the stock solution in DMEM/F12 medium 1% fetal bovine serum (Hyclone), 100 U/mL penicillin, 100 $\mu\text{g}/\text{mL}$ streptomycin, and 2 mM L-glutamine (400 μl of stock solution into 200 mL of media to make 1 μM ^{14}C -MPS/ ^{14}C -MPO media solution). In preliminary experiments, cells were exposed to 1 μM ^{14}C -MPS/ ^{14}C -MPO at 37 $^{\circ}\text{C}$ for 0, 8, 16, 24, 48, and 72 h in a 96-well plate (2 μL media in each well). At the determined time points, culture media was removed and the cells were washed with ice cold PBS (3 \times 1 mL) to remove residual ^{14}C -MPS or ^{14}C -MPO and placed in a scintillation vial. To the remaining washed cells was added 5 mL of ice cold PBS and the cells removed using a cell scraper, and transferred to centrifuge tubes. Each well was washed an additional time with PBS to remove residual cells. Cells were centrifuged for 5 min and supernatant was transferred to a scintillation vial. Cells were treated with lysis buffer containing 20 mM Tris-HCl (pH 7.5), 150 mM NaCl, 1 mM Na_2EDTA , 1 mM EGTA, 1% Triton-X-100, 2.5 mM sodium pyrophosphate, 1 mM beta-glycerophosphate and 1 mM Na_3VO_4 (Cell Signaling Technology, Beverly, MA). Additions to the lysis solution were made to give final concentrations of 0.5% Na-deoxycholate, 0.5% SDS, 1 μM okadaic acid, 1 mM phenylmethylsulfonyl (PMSF), 0.1 mg/mL benzamidine, 8 $\mu\text{g}/\text{mL}$ calpain inhibitors I and II and 1 $\mu\text{g}/\text{mL}$ each leupeptin, pepstatin A and aprotinin. Lysis buffer (500 μl) was added to the cell pellet and vortexed. After 30 min, the cell lysate was centrifuged and the supernatant containing the cytosolic fraction was separated. Scintillation fluid was added to all samples to obtain a standard volume and total counts (cpm) were recorded. Data was collected in triplicate for each time point. The total amount of OP inside cells was calculated using the following equation and was plotted against OP exposure time (Figure 5).

$$\text{Total amount of OP inside cells (nM)} = \frac{[\text{Total radioactivity inside cells (cpm)} \times \text{Initial OP concentration (nM)}]}{[\text{Total radioactivity in media (cpm)} + \text{Total radioactivity inside cells (cpm)}]}$$

Fate of ^{14}C -MPS and ^{14}C -MPO in uptake experiments

In order to determine the fate of ^{14}C -MPS and ^{14}C -MPO in media during uptake experiment and the amounts of MPS/MPO and their degradation products in cell cytosol, uptake

experiments were performed at 24, 48 and 72 h in a petri-dish plate (20 mL media in each plate; 1 μM ^{14}C -MPS or ^{14}C -MPO) using a similar protocol to the previous section. After harvesting cells, total cell numbers were calculated by trypan blue counting. After cell lysis, cytosolic fraction was collected and was loaded on preparative silica gel G₂₅₄ TLC plate and reference standards of cold MPS and MPO spotted at the corner of the plate. TLC plates were eluted using EtOAc:hex (1:1). The radioactive bands were identified by correlation with standards, removed and collected in individual liquid scintillation vials. Similarly, 100 μL of media was also loaded on TLC plate and bands were collected. Scintillation fluid was added to all samples to obtain a standard volume and total counts (cpm) were recorded. Data was collected in triplicate for each time point. Concentrations of OP in cell cytosol per million cells were calculated using the following equation and plotted against OP exposure time (Figure 6).

$$\text{nM OP in cytosol}/10^6 \text{ cells} = \frac{\text{Radioactivity for OP or its degradation product in cytosol (cpm)} \times \text{Initial OP concentration (nM)}}{[\text{Total radioactivity in media (cpm)} + \text{Total radioactivity inside cells (cpm)}] \times \text{Number of cells (in millions)}}$$

The partition coefficient values (media-cell) for the OPs and their degradation products were calculated by dividing the amount of ^{14}C -MPS/ ^{14}C -MPO in cell cytosol by amount in the media at 48 h exposure time. The uptake rate constant was calculated from the negative slope of the plot between $\ln(\text{nM increment of OP in cytosol})$ vs. OP exposure time (h).

Results

Synthesis of ^{14}C -Methyl Paraoxon (^{14}C -MPO)

^{14}C -Methyl parathion (1 mCi) with a specific activity of 41.65 mCi/mmol was oxidized with meta-chloroperoxybenzoic acid (*m*-CPBA) in methylene chloride to yield ^{14}C -MPO. Purification was conducted using preparative thin layer chromatography (prep-TLC). The radioactive yield of ^{14}C -MPO was 0.360 mCi and the radiochemical purity of both ^{14}C -MPS and ^{14}C -MPO were > 98% (Figure 2). Radioactive MPS and MPO structures were confirmed by co-elution on TLC with standard (cold) MPS and MPO, which were characterized by NMR and MS.

Viability of SH-SY5Y Cells Exposed to ^{14}C -MPS and ^{14}C -MPO

SH-SY5Y cells were treated with ^{14}C -MPS or ^{14}C -MPO ranging from 10 nM to 100 μM and the cell viability assessed by MTT assay. Some cytotoxicity was observed with both MPS and MPO at 50 μM at time points 48 and 72 h and at least 60% cytotoxicity occurred at all time points when the cells were exposed to 100 μM except MPS treatment for 24 h (Figure 3) that showed no significant decrease in viability. At 100 μM concentration, MPS showed 4% (24 h), 60% (48 h) and 90% (72 h) cytotoxicity, respectively while MPO showed more than 80% cytotoxicity after just 24 h.

Stability of ^{14}C -MPS and ^{14}C -MPO in Culture Media

The stability of ^{14}C -MPS and ^{14}C -MPO in culture media was determined by incubating 1 μM of the OP in tissue culture media at 37 $^{\circ}\text{C}$ for up to 120 h. The media was analyzed at various time points by prep-TLC and the amount of OP and degradation products was quantified by radioactivity counting of isolated bands. The major degradation pathways for ^{14}C -MPS and ^{14}C -MPO are oxidation/hydrolysis and hydrolysis, respectively (Figure 7) forming the water soluble DMTP and DMP as primary metabolites. The formation of DMTP and DMP from paraoxon and like compounds are well documented (26,27). ^{14}C -MPS

and ^{14}C -MPO showed similar stability profiles. After 72 h of incubation in media more than 50% of ^{14}C -MPS (Figure 4A) and ^{14}C -MPO (Figure 4B) were recovered from the media unchanged. Both ^{14}C -MPS and ^{14}C -MPO hydrolyzed with loss of the p-nitrophenol group to yield dimethyl thiophosphoric acid (thiophosphate) and dimethylphosphate (phosphoric acid) (Figure 7), respectively, as determined by co-elution with standards. ^{14}C -MPS was found to be relatively stable to oxidation in media and formed less than 1% ^{14}C -MPO after 4 days (Figure 4A). Based on isolation and measurement of the eluted bands, 80–97% and 78–95% of the originally applied amount of ^{14}C -MPS and ^{14}C -MPO were recovered. The rate constant for degradation (hydrolysis) of ^{14}C -MPS and ^{14}C -MPO were calculated to be $7.0 \times 10^{-3} \text{ h}^{-1}$ and $6.0 \times 10^{-3} \text{ h}^{-1}$, respectively. The half lives for ^{14}C -MPS and ^{14}C -MPO in media were 91.7 h and 101.9 h, respectively.

Uptake of ^{14}C -MPS and ^{14}C -MPO in SH-SY5Y Human Neuroblastoma Cells

Using the cell viability and media stability data, time points up to 96 h and OP concentrations of $1 \mu\text{M}$ were chosen for uptake studies since little to no loss of cells were observed under these conditions. In preliminary uptake experiments, cells were exposed to $1 \mu\text{M}$ of ^{14}C -MPS and ^{14}C -MPO for different exposure times *viz.* 0, 8, 12, 24, 48, 72 and 96 h. A comparative plot of uptake for ^{14}C -MPS and ^{14}C -MPO is shown in Figure 5 indicating that MPO achieved a maximum level of 46 nM at the 48 hr time point and MPS a 13 nM maximum at 24 h. At the most, only 5% (approx. 8000 cpm; Appendix) of the total applied radioactivity (170,000 cpm) of either MPS or MPO entered the cells.

In order to determine the fate of ^{14}C -MPS and ^{14}C -MPO in media during the uptake experiments and the total amount of MPS, MPO and/or the degradation products in cell cytosol, uptake experiments were performed at 24, 48 and 72 h (Figure 6A–D). At each time point, a sample of the cytosolic fraction and the media was loaded on preparative TLC plate, the OPs separated, and analyzed to determine the stability of ^{14}C -MPS or ^{14}C -MPO and formation of the hydrolysis products during the uptake experiment (Table 1 and 2). ^{14}C -MPS and ^{14}C -MPO were stable in media throughout the uptake experiment. The cell counts for both experiments were normalized and values of ^{14}C -MPS and ^{14}C -MPO uptake were reported per one million cells. As found in the preliminary uptake experiment (Figure 5), the total amount of MPO uptake (sum of MPO and its degradation product) was greater than the total MPS uptake (sum of MPS and its degradation products) (Figure 6A). It was interesting to note that in case of ^{14}C -MPO uptake, a large amount of the hydrolyzed product, dimethyl phosphate (80–90% of total radioactivity inside cells) (Figure 6C) was found in cells while a greater amount of ^{14}C -MPS was found inside cells compared with its degradation products, MPO and DMTP (Figure 6B).

The maximum radioactivity inside cells was reached after 48 h of ^{14}C -MPS/ ^{14}C -MPO exposure with a total uptake of 1.19 and 1.76 nM/ 10^6 cells for MPS and MPO, respectively while the actual amounts of MPS and MPO inside cells after 48 h exposure time were 0.54 and 0.37 nM/ 10^6 cells (Table 1), respectively. Based on TLC analysis, in case of ^{14}C -MPS uptake, the ratio of ^{14}C -MPS to that of degradation products inside cells was 46:38:16 (MPS:MPO:DMTP) at 48 h exposure time while the uptake of MPO showed an MPO:DMO ratio of 21:79 (MPO: DMP) (Table 1).

The amount of ^{14}C -MPS and ^{14}C -MPO determined inside cells at various exposure times (Figure 6D) shows that a larger amount of ^{14}C -MPS entered cells than ^{14}C -MPO at each time point and only a negligible amount of ^{14}C -MPS or ^{14}C -MPO was found to be associated with the membrane fraction. The percent total recovery of all label in the uptake experiments for ^{14}C -MPS and ^{14}C -MPO were found to be > 92% and > 95%, respectively. The cells-media partition coefficients (K_d) were calculated to be 6.3×10^{-4} and 5.9×10^{-4} with uptake rate constants of 0.054 h^{-1} and 0.025 h^{-1} for MPS and MPO, respectively.

Discussion

In this study, the stability, uptake and cytotoxicity of ^{14}C -methyl parathion and ^{14}C -methyl paraoxon were tested in a SH-SY5Y human neuroblastoma cell line. The radiolabel was placed at both methoxy groups so that attachment of the OP to biomolecules and the formation of hydrolysis products could be tracked more efficiently as compared to studies in which the radiolabel was incorporated at the *p*-nitrophenoxy group (26,28–30). Synthesis of radiolabeled paraoxon from $(^{14}\text{C}\text{H}_3\text{O})_2$ -parathion was accomplished in greater than 98% chemical and radiochemical purity. The specific activity was 41.65 mCi/mmol as determined by chromatography.

Stability studies in culture media indicated that more than 50% of either ^{14}C -MPS or ^{14}C -MPO remained in the media after 72 h (Figure 4). The degradation pathways expected for ^{14}C -MPS was oxidation/hydrolysis and for ^{14}C -MPO hydrolysis was anticipated (Figure 7). However, we did not observe oxidation of ^{14}C -MPS to ^{14}C -MPO in culture media. Thus, hydrolysis, or loss of the *p*-nitrophenoxy group, to yield dimethyl thiophosphate (DMTP) was the major degradation route for ^{14}C -MPS in the culture media. Direct formation of DMTP from MPS has been previously reported (26,27,31–33). In contrast, a significant amount of ^{14}C -MPO was found in cell lysates following ^{14}C -MPS treatment indicative of the greater conversion of MPS to MPO in cells (Figure 6B).

To ensure that the uptake studies were conducted with continued viability during the course of the exposure, the cytotoxicity was next examined. As expected, the more reactive phosphorylating agent ^{14}C -MPO was more cytotoxic than ^{14}C -MPS at concentration above 10 μM (Figure 3). As a result of this data, we chose a concentration of MPS and MPO (1 μM) that was below the cytotoxic threshold in order to examine differences in uptake of these OP's in viable cells.

Although a 20-fold difference in the lipophilicity of MPS and MPO exists, this structural difference did not result in equally dramatic change in cellular uptake, in fact, our initial uptake results showed that uptake was not related to the lipophilicity. Our experiments showed that the hydrolysis product of MPO, dimethyl phosphate (DMP), actually accounted for a higher overall amount of radioactivity in MPO treated cells as compared with MPS treated cells indicating relatively equal access by MPO and MPS. However, a greater overall amount of MPS was found inside cells than MPO. The greater amount of MPS than MPO found in cells could be the result of the greater stability of MPS once inside the cell and/or rapid breakdown of MPO in cells to DMP thereby reducing the net amount of MPO found. The higher amount of DMP found in cells could be due to the intracellular hydrolysis and metabolism of MPO and/or extracellular (media-mediated) metabolism followed by passive diffusion across the cell membrane (34). Although a maximum cellular uptake of OP's was not more than 5% of total OP exposure (1 μM) it is noteworthy that uptake was concentration dependent as observed from the results of lower concentration (100 nM and 10 nM) uptake experiments.

The cytotoxicity induced in the ^{14}C -MPS treated cells followed a delayed trend similar to that in the ^{14}C -MPO treated cells after 24 h of exposure likely due to a rate-dependent oxidative conversion. The highest amount of cytotoxicity (90%) exhibited by MPS was at 100 μM concentration after 72 h of exposure time. Although very little ^{14}C -MPO (7–10%, Table 2) was found in the media, a significant amount of ^{14}C -MPO (33–37%, Table 1) was found in the cytosol in MPS-treated cells. Therefore, it is likely that conversion from MPS to MPO contributed to the cytotoxicity (16).

In conclusion, differences in the stability, uptake and cytotoxicity of ^{14}C -MPS and ^{14}C -MPO in SH-SY5Y human neuroblastoma cells were found. The use of dual-labeled MPS

and MPO allowed for precise intracellular measurements of parent and hydrolyzed product and for determining rate comparisons. Data obtained in this work suggests that the thionate MPS and the oxon MPO access cells at different rates and to different extents that could yield distinct differences in protein responses.

Supplementary Material

Refer to Web version on PubMed Central for supplementary material.

Acknowledgments

We thank Sarah Ulatowski for her help with the cell experiments. The authors thank the NIH for grant support (UO1-ES016102) and SBIR awards to ATERIS Technologies LLC (R43 ES016392 and U44 NS058229). Support for the Core Laboratory for Neuromolecular Production (NIH P30-NS055022) and the Center for Structural and Functional Neuroscience (NIH P20-RR015583) is appreciated.

Abbreviations used

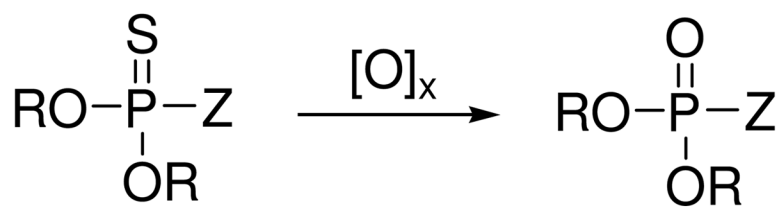
MPO	methylparaoxon
MPS	methyl parathion
DMP	dimethylphosphate
DMTP	dimethylthiophosphate

Literature Cited

1. Bajgar J. Organophosphates/nerve agent poisoning: mechanism of action, diagnosis, prophylaxis, and treatment. *Adv Clin Chem.* 2004; 38:151–216. [PubMed: 15521192]
2. Costa LG. Current issues in organophosphate toxicology. *Clin Chim Acta.* 2006; 366:1–13. [PubMed: 16337171]
3. DuBois KP, Doull J, Salerno PR, Coon JM. Studies on the toxicity and mechanisms of action of p-nitrophenyl diethyl thionophosphate (Parathion). *J Pharmacol Exp Ther.* 1949; 95:79–91. [PubMed: 18111480]
4. Forsyth CS, Chambers JE. Activation and degradation of the phosphorothionate insecticides parathion and EPN by rat brain. *Biochem Pharmacol.* 1989; 10:1597–1603. [PubMed: 2730675]
5. Gage JC. A cholinesterase inhibitor derived from O, O-diethyl O-p-nitrophenyl thiophosphate in vivo. *Biochem J.* 1953; 54:426. [PubMed: 13058919]
6. Levi PE, Hollingworth RM, Hodgson E. Differences in oxidative dearylation and desulfuration of fenitrothion by cytochrome P-450 isoenzyme and in the subsequent inhibition of monooxygenase activity. *Pestic Biochem Physiol.* 1988; 32:224–231.
7. Sultatos LG, Minor LD. Biotransformation of paraoxon and p-nitrophenol by isolated perfused mouse livers. *Toxicology.* 1985; 36:159–169. [PubMed: 4049428]
8. Wang C, Murphy SD. Kinetic analysis of species difference in acetylcholinesterase sensitivity to organophosphate insecticides. *Toxicol Appl Pharmacol.* 1982; 66:409–419. [PubMed: 7167968]
9. Ballantyne, B.; Marrs, T. *Clinical and experimental toxicology of organophosphates and carbamates.* Butterworth Heinemann; Boston: 1992.
10. Broomfield, CA.; Millard, CB.; Lockridge, O.; Caviston, TL. *Enzymes of the cholinesterase family.* Plenum Press; New York: 1995.
11. Fukuto TR. Mechanism of action of organophosphorus and carbamate insecticides. *Environ Health Perspect.* 1990; 87:245–254. [PubMed: 2176588]
12. Carlson K, Ehrich M. Organophosphorus compound-induced modification of SH-SY5Y human neuroblastoma mitochondrial transmembrane potential. *Toxicol Appl Pharm.* 1999; 160:33–42.
13. Carlson K, Jortner BS, Ehrich M. Organophosphorus compound-induced apoptosis in SH-SY5Y human neuroblastoma cells. *Toxicol Appl Pharm.* 2000; 168:102–113.

14. Ehrich M, Correll L, Veronesi B. Acetylcholinesterase and neuropathy target esterase inhibitions in neuroblastoma cells to distinguish organophosphorus compounds causing acute and delayed neurotoxicity. *Fund Appl Toxicol.* 1997; 38:55–63.
15. Greenman SB, Rutten MJ, Fowler WM, Scheffler L, Shortridge LA, Brown B, Sheppard BC, Deveney KE, Deveney CW, Trunkey DD. Herbicide/pesticide effects on intestinal epithelial growth. *Environ Res.* 1997; 75:85–93. [PubMed: 9356197]
16. Saleh AM, Vijayasathya C, Fernandez-Cabezudo M, MT, Petroianu G. Influence of Paraoxon (POX) and Parathion (PAT) on Apoptosis: a Possible Mechanism for Toxicity in Low-dose Exposure. *J Appl Toxicol.* 2003; 23:23–29. [PubMed: 12518333]
17. Veronesi B, Ehrich M. Using neuroblastoma cell lines to examine organophosphate neurotoxicity. *In Vitro Toxicol.* 1993; 6:57–65.
18. Nishio A, Uyeki EM. Induction of sister chromatid exchanges in Chinese hamster ovary cells by organophosphate insecticides and their oxygen analogs. *J Toxicol Environ Health.* 1981; 8:939–946. [PubMed: 7338954]
19. Tuler SM, Bowen JM. Toxic effect of organophosphates on nerve cell growth and ultrastructure in culture. *J Toxicol Environ Health.* 1989; 27:209–223. [PubMed: 2733059]
20. Antunes-Madeira MC, Videira RA, Madeira VMC. Effects of parathion on membrane organization and its implications for the mechanisms of toxicity. *Biochim Biophys Acta.* 1994; 1190:149–154. [PubMed: 8110808]
21. Casida JE, Quistad GB. Organophosphat toxicology: Safety aspects of nonacetylcholinesterase secondary targets. *Chem Res Toxicol.* 2004; 17:983–998. [PubMed: 15310231]
22. Casida JE, Quistad GB. Serine hydrolase targets of organophosphorus toxicants. *Chem Biol Interact.* 2005; 157–158:277–283.
23. Food and Agriculture Organization of the United Nations: United Nations Environment Programme (UNEP/FAO/RC/CRC.1/19/Add.4). 2005. Monograph, *Methyl parathion: Supporting documentation from the European Community.*
24. Czerwinski SE, Maxwell DM, Lenz DE. A method for measuring octanol: water partition coefficients of highly toxic organophosphorus compounds. *Toxicol Mechanisms and Methods.* 1998; 8:139–149.
25. Ross RA, Spengler BA, Biedler JL. Coordinate morphological and biochemical interconversion of human neuroblastoma cells. *J Natl Cancer Inst.* 1983; 71:96–99.
26. Abu-Qare AW, Abdel-Rahman AA, Kishk AM, Abou-Donia MB. Placental transfer and pharmacokinetics of a single dermal dose of [14C]methyl parathion in rats. *Toxicol Sci.* 2000; 53:5–12. [PubMed: 10653515]
27. Panuwet P, Prapamontol T, Chantara S, Thavornnyuthikarn P, Bravo R, Restrepo P, Walker RD, Williams BL, Needham LL, Barr DB. Urinary parnitrophenol, a metabolite of methyl parathion in Thai farmer and child populations. *Arch Environ Contam Toxicol.* 2009; 57:623–629. [PubMed: 19365648]
28. Frosta M, Abo-El-Seoud MA. Fate and metabolism of [14C] parathion -methyl as examined by soybean and wheat cell cultures. *Sci Total Environ.* 1993; 134:681–687.
29. Lichtenstein EP, Fuhremann TW, Abraham AH, Zahlten RN, Stratman FW. Metabolism of [14C]Parathion and [14C]Paraoxon with fractions and subfractions of rat liver cells. *J Agric Food Chem.* 1973; 21:416–424. [PubMed: 4708807]
30. Abu-Qare AW, Abdel-Rahman AA, Ahmad H, Kishk AM, Abou-Donia MB. Absorption, distribution, metabolism and excretion of daily oral doses of [14C]methyl parathion in hens. *Toxicol Lett.* 2001; 125:1–10. [PubMed: 11701217]
31. Hernandez F, Sancho JV, Pozo OJ. An estimation of the exposure to organophosphorus pesticides through the simultaneous determination of their main metabolites in urine by liquid chromatography–tandem mass spectrometry. *J Chromat B.* 2004; 808:229–239.
32. Sharmila M, Ramanand K, Sethunathan N. Hydrolysis of methyl parathion in a flooded soil. *Bull Environ Contam Toxicol.* 1989; 43:45–51. [PubMed: 2758139]
33. Hernandez F, Sancho JV, Pozo OJ. Direct determination of alkyl phosphates in human urine by liquid chromatography/electrospray tandem mass spectrometry. *Rapid Commun Mass Spectrom.* 2002; 16:1766–1773. [PubMed: 12207365]

34. Borowitz SM, Ghishan FK. Phosphate transport in human jejunal brush-border membrane vesicles. *Gastroenterology*. 1989; 96:4–10. [PubMed: 2909436]



**1: phosphorothionate
insecticide**

2: oxon

Figure 1.

Structures of representative phosphorothionates insecticides and the corresponding oxons. Malathion (R = Me, Z = -SCH(CO₂Et)CH₂CO₂Et), parathion (R = Et, Z = -OPh-p-NO₂), methyl parathion (R = Me, Z = -OPh-p-NO₂), chlorpyrifos (R = Et, Z = O-2,3,5-trichloropyridinol), and diazinon (R = Et, Z = O[6-Me, 4-iPr-pyrimidinol]).

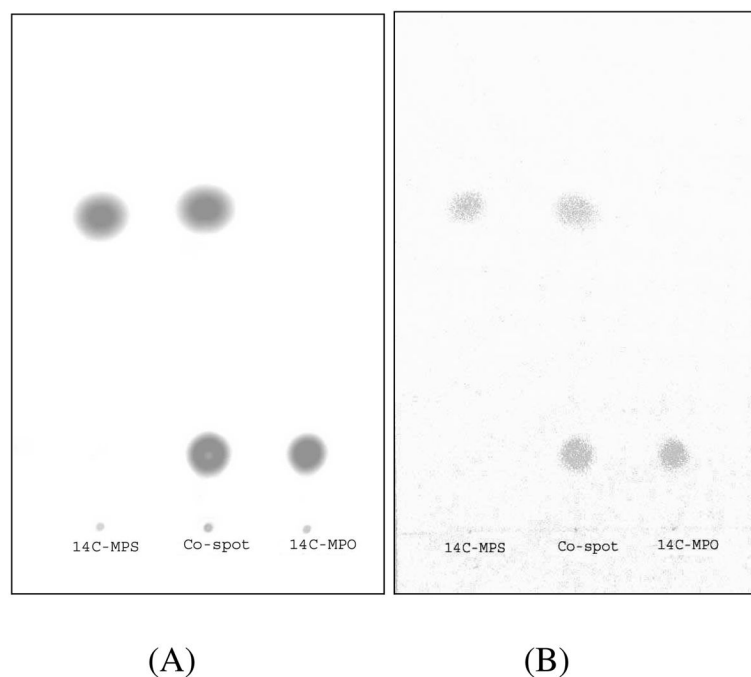


Figure 2. Thin layer chromatographic analyses of ^{14}C -MPS and ^{14}C -MPO (EtOAc:hex, 1:1). (A). Radioactivity image. (B) UV image. R_f of MPS = 0.65 and MPO = 0.18.

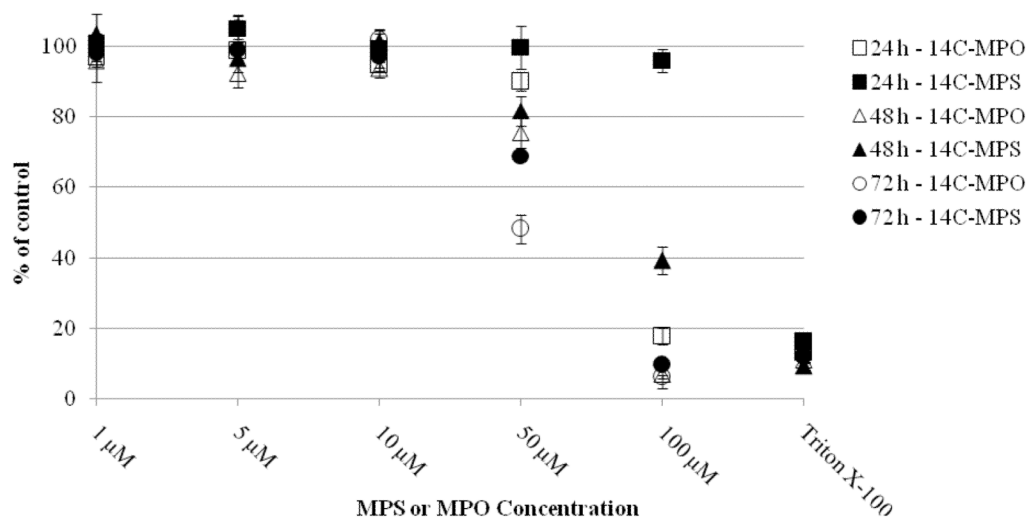


Figure 3. Cytotoxic effect of ^{14}C -MPS and ^{14}C -MPO on SH-SY5Y cells. Cells were treated with various concentrations of ^{14}C -MPS and ^{14}C -MPO for 24, 48 and 72 h. Cell viability was determined by 3-[4, 5-dimethylthiazol-2-yl]-2, 5-diphenyl tetrazolium bromide (MTT) assay. (a) SH-SY5Y cell viability following 24 h exposure to ^{14}C -MPS and ^{14}C -MPO; (b) SH-SY5Y cell viability following 48 h exposure to ^{14}C -MPS and ^{14}C -MPO; (c) SH-SY5Y cell viability following 72 h exposure to ^{14}C -MPS and ^{14}C -MPO. Results are presented as % of vehicle control, determined by comparing the absorbance readings of the wells containing the OP treated cells with those of the vehicle (0.1% acetonitrile) treated cells. Data represent the mean \pm SEM ($n = 8$). Triton X-100 was used as a positive control (= 100% cell death).

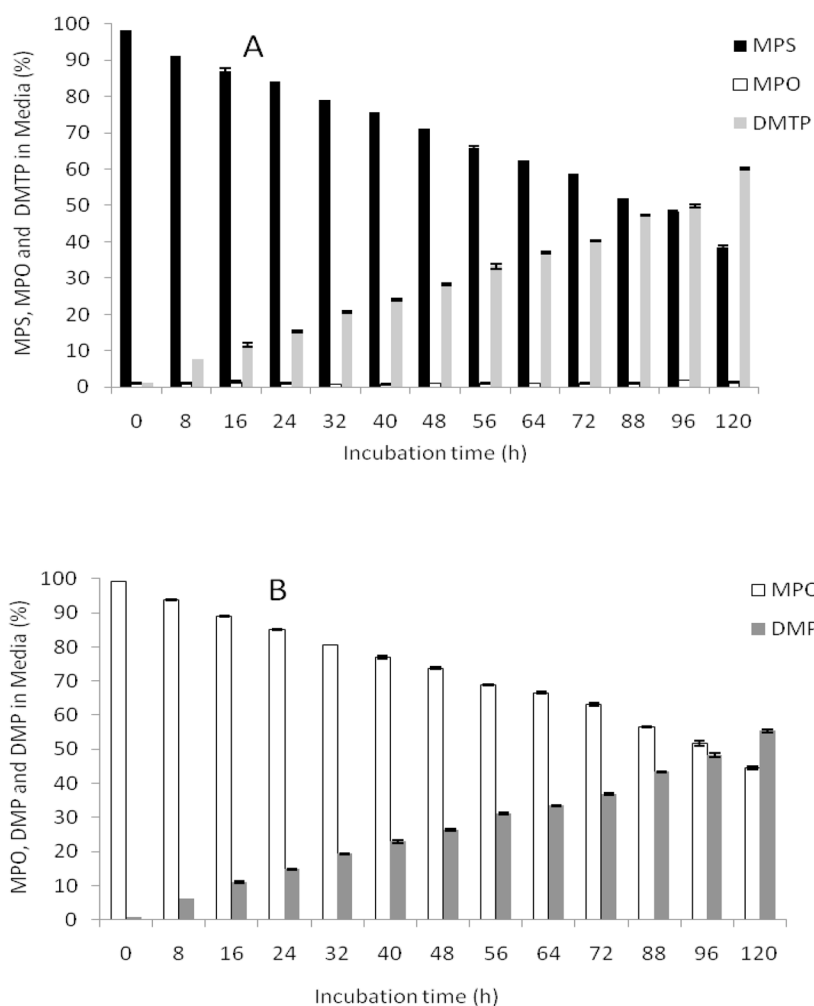


Figure 4. Stability of radiolabeled MPS or MPO in 1% FBS culture media. (A) ^{14}C -MPS. (B) ^{14}C -MPO. Data represents mean \pm SEM ($n = 3$). ^{14}C -DMTP and ^{14}C -DMP are primary metabolites of ^{14}C -MPS and ^{14}C -MPO hydrolysis.

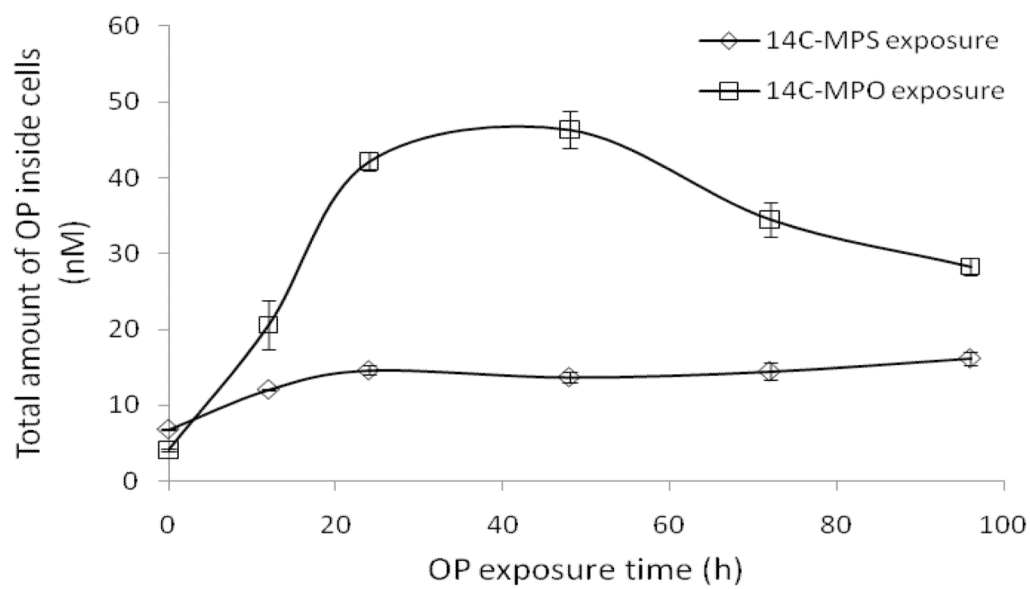


Figure 5. Uptake of ^{14}C -MPS or ^{14}C -MPO into SH-SY5Y cells at different exposure times (0, 12, 24, 48, 72 and 96 h). Data represents mean \pm SEM ($n = 3$).

Figure 6 (AB).

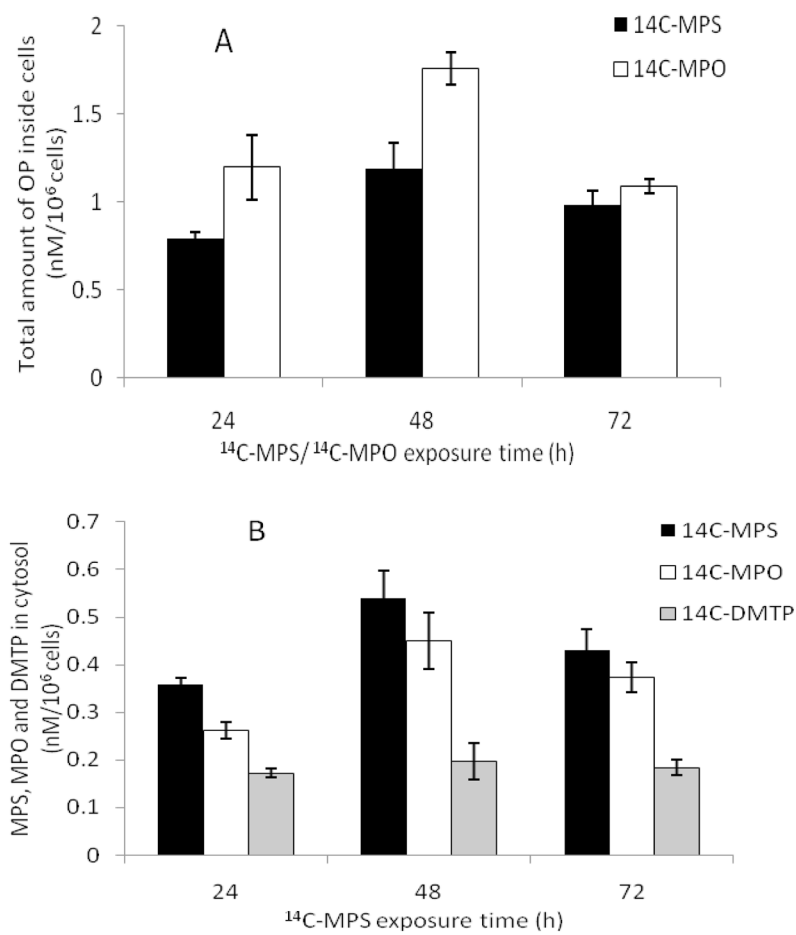


Figure 6 (CD).

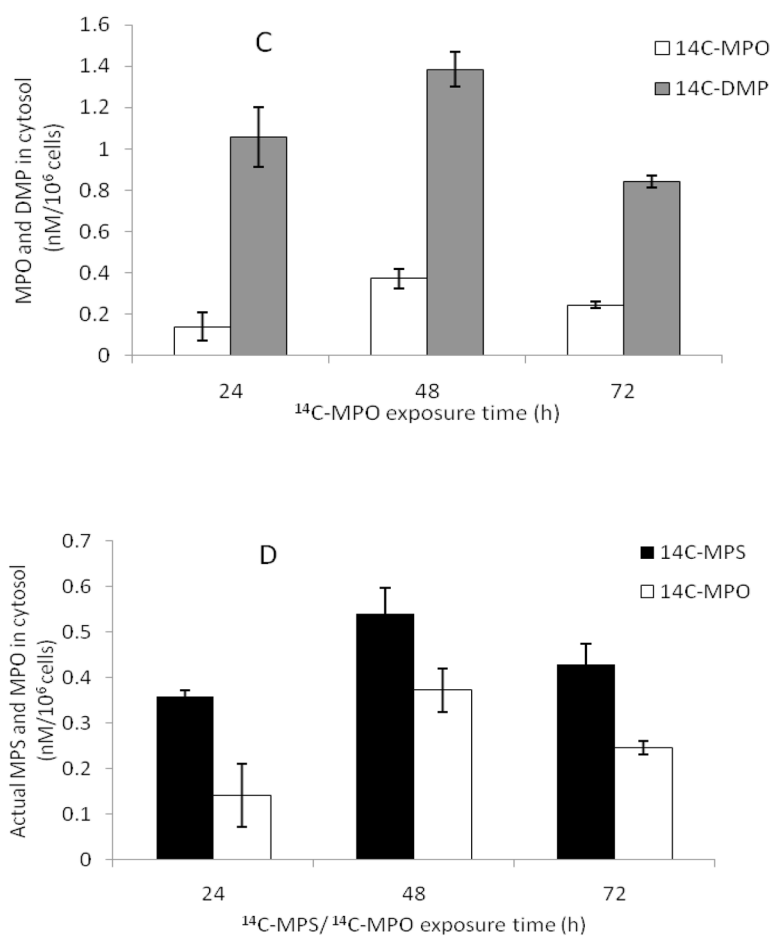


Figure 6. Uptake of ¹⁴C-MPS or ¹⁴C-MPO in SH-SY5Y cells at different exposure times. Cell numbers per experiment were normalized and uptake values are indicated for 10⁶ cells. (a) Total radioactivity (OP and their degradation products) found inside cells following exposure to 1 μM MPS or MPO; (b) Uptake of ¹⁴C-MPS (1 μM) and its degradation products; (c) Uptake of ¹⁴C-MPO (1 μM) and its degradation product; (d) Amount of ¹⁴C-MPS/¹⁴C-MPO found inside cells at 100 nM. Data represents mean ± SEM (n = 3). ¹⁴C-DMTP and ¹⁴C-DMP are primary metabolites of ¹⁴C-MPS and ¹⁴C-MPO hydrolysis.

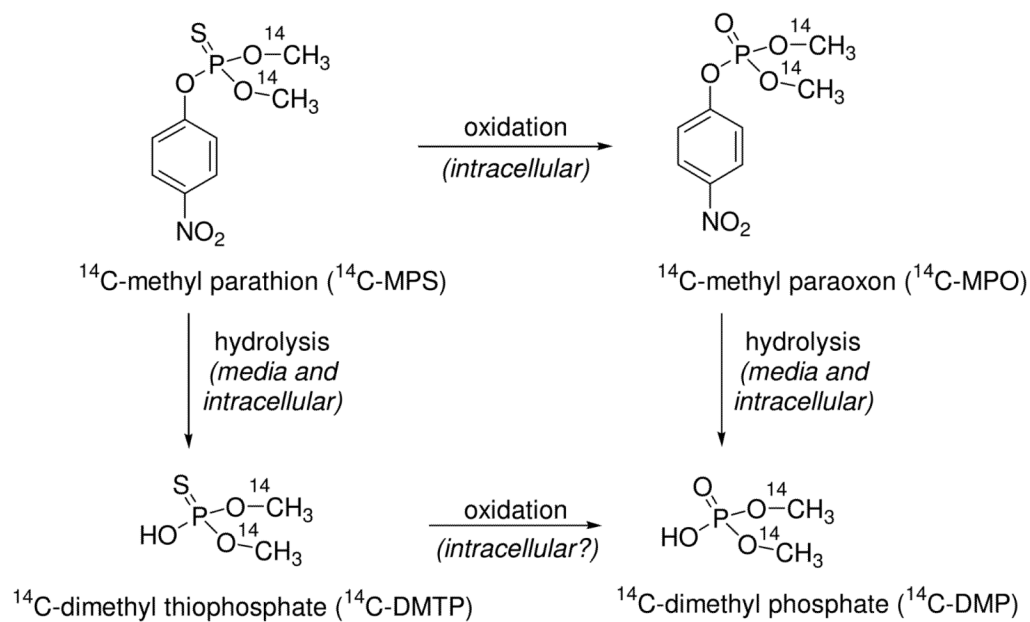


Figure 7. Degradation (hydrolysis) of ^{14}C -methyl parathion and ^{14}C -methyl paraoxon in media.

Table 1

Percentage of MPS, MPO, DMTP and/or DMP in cell cytosol after exposure of cells to 1 μ M of OP (MPS or MPO)¹

Incubation time (h)	Percentage of MPS, MPO, DMTP and/or DMP in cell cytosol (per 10 ⁶ cells) ²			Relative Ratio's		
	MPS	MPO	DMP and/or DMTP	MPS	MPO	DMP and/or DMTP
	¹⁴ C-MPS					
24	0.036 \pm 0.001	0.026 \pm 0.002	0.017 \pm 0.001	45.3 \pm 1.5	33.0 \pm 0.9	21.7 \pm 0.6
48	0.054 \pm 0.006	0.045 \pm 0.006	0.020 \pm 0.004	45.8 \pm 2.0	37.9 \pm 1.7	16.3 \pm 1.1
72	0.043 \pm 0.004	0.037 \pm 0.003	0.018 \pm 0.002	43.5 \pm 1.8	37.9 \pm 2.3	18.7 \pm 0.6
	¹⁴ C-MPO					
24	-	0.014 \pm 0.007	0.106 \pm 0.014	-	10.9 \pm 4.5	89.1 \pm 4.5
48	-	0.037 \pm 0.005	0.139 \pm 0.008	-	21.2 \pm 2.3	78.8 \pm 2.3
72	-	0.025 \pm 0.002	0.084 \pm 0.003	-	22.5 \pm 0.7	77.5 \pm 0.7

¹ Ratios of OP and their degradation products were determined by preparative TLC analysis;

² Data represents mean \pm SEM (n = 3).

Table 2

Relative ratio's of MPS, MPO, DMTP and/or DMP in culture media after exposure of cells to 1 μ M of OP (MPS or MPO)¹

Incubation time (h)	Relative Ratio's ²		
	MPS	MPO	DMP and/or DMTP
	¹⁴ C-MPS		
24	74.3 \pm 1.0	9.8 \pm 1.0	16.0 \pm 0.2
48	63.9 \pm 0.1	6.8 \pm 0.9	29.3 \pm 0.9
72	52.9 \pm 0.8	10.3 \pm 1.4	36.8 \pm 1.6
	¹⁴ C-MPO		
24	-	69.7 \pm 3.3	30.3 \pm 3.3
48	-	62.5 \pm 0.6	37.5 \pm 0.6
72	-	61.4 \pm 0.2	38.6 \pm 0.2

¹Ratios of OP and their degradation products were determined by preparative TLC analysis;

²Data represents mean \pm SEM (n = 3).